Significant Structure Change in Nonequimolar Complexes of Poly(ethylenimine) and Octadecanoic Acid Induced by Polymer Backbone Branching

Biye Ren, Zhiyu Cheng, Zhen Tong,* Xinxing Liu, Chaoyang Wang, and Fang Zeng

Research Institute of Materials Science, South China University of Technology, Guangzhou 510640, China

ABSTRACT: To illustrate the effect of polymer backbone branching on the crystal and mesomorphous structures of polyelectrolyte−amphiphile complexes, the complex of branched poly(ethylenimine) (*b*PEI) and octadecanoic acid (OA), *b*PEI−OA-*x*, where *x* is the mole ratio of OA to amino group, was investigated with WAXD, SAXS, FTIR, DSC, and polarized optical microscope. The corresponding results from the complexes of linear poly-(ethylenimine) (*l*PEI) and OA, *l*PEI−OA-*x* with *x* < 1 were taken as the reference. The bound OA alkyl tails form the hexagonal crystal phase (α_H) in the *b*PEI−OA complex as opposed to the less symmetric triclinic phase (β_T) in the *l*PEI−OA complex. The alkyl chains of bound OA molecules in both crystal phases were interdigitated and the long period of the mesomorphous layer was 3.1 nm for the *b*PEI−OA, longer than 2.8 nm for the *l*PEI−OA owing to less dense stacking in the former. Thermal stability of all the complexes was enhanced compared with the pure OA due to the strong electrostatic attraction between −COO$^-$ from OA and −NH$_2^+$ or −NH$_3^+$ from PEI. An ionic thermotropic liquid crystal phase of smectic B was found at temperatures above the melting point of the OA tail crystal, but the isotropic transition temperature T_i of the *b*PEI−OA complexes was higher by ca. 20 °C than that of the *l*PEI−OA complexes due to higher symmetry of the α_H phase in the *b*PEI−OA tail chain crystal. The present results have demonstrated for the first time that the branching of polyelectrolyte backbone can tune the crystal and mesomorphous structures of polyelectrolyte−amphiphile complexes in addition to the complex composition.

1. Introduction

In recent years, polymer−amphiphile complexes based on specific noncovalent interactions, such as hydrogen bonding, charge transfer, ionic interactions, or coordination complexation, have received considerable attention due to the simple fabrication, interesting properties, and potential applications.[1−5] Polymer−amphiphile complexes, like comb-shape polymers, usually form different mesomorphous stacking structures with various phases of side-chain crystal and/or liquid-crystal by the bound alkyl chains, which provides unique possibility to tailor the morphology and properties.[2−8]

Highly branched poly(ethylenimine) (*b*PEI) is a water-soluble polymer and widely used in the medical and paper industries.[9,10] Ultrathin polymer films with well-defined molecular architecture and various potential applications have been fabricated through the layer-by-layer deposition of *b*PEI with oppositely charged polyelectrolytes.[11] *b*PEI has been also used for preparing the Langmuir−Blodgett monolayer or multilayer films with various *n*-alkanoic acids.[12] Recently, the complexes of *b*PEI and *n*-alkanoic acids with the lamellar mesomorphous structure have been reported.[13,14] The long period of the complex and the tendency to crystallize of the tail chains were found to depend on the tail length of the bound *n*-alkanoic acids. For example, Thünemann[15] reported that complexes of *b*PEI and perfluorinated carboxylic acids possessed two lamella phases of α and β with low surface tension, depending on the chain length of the perfluorinated carboxylic acid. The partially crystalline lamella structure was also observed from the complexes of *b*PEI and *n*-alkanoic acids (*n* = 10−26). Chen and Hsiao[16] investi-

gated the complexes of *b*PEI and dodecylbenzenesulfonic acid (DBSA) with wide range of DBSA contents and found the thermotropic liquid crystal phase in these *b*PEI-DBSA complexes. Zhou et al.[17] revealed a reversible crystalline phase transition of the tail chains with changing temperature for a series of *b*PEI−octadecanoic acid (OA) complexes (*b*PEI(OA)$_x$) with *x* = 0.6−1.67 (where *x* represents the mole ratio of OA to amino group in *b*PEI). In a previous study, we prepared a series of complexes of *b*PEI and perfluorooctanoic acid (PFOA) with various compositions, which showed a change in supramolecular lamella stacking from the bilayer to monolayer with increasing PFOA content.[18]

Recently, we have systemically investigated the structure change in the nonequimolar complexes of linear poly(ethylenimine) and octadecanoic acid, *l*PEI−OA-*x*, with different compositions *x* = 0.66−1.45.[19] Two crystalline modifications β_O (β-orthorhombic) and β_T (β-triclinic) were found for the bound OA tails to exist in the complexes varying with *x* and only 8−10 CH$_2$ groups in an OA molecule participated in the crystal. The complexes of *x* > 1.0 were predominant with the β_O form and stacked into an end-to-end bilayer lamella. While for the complexes of *x* < 1.0, the β_T form was dominant and stacked in an interdigitating monolayer structure. The thermotropic liquid crystal was observed only from the complexes of *x* < 1.0 above the melting point of the OA tail crystal. These results indicate that the supramolecular structure of polyelectrolyte−amphiphile complexes can be effectively tuned by changing the relative amount of bound amphiphiles. In other words, the amount of added amorphous polyelectrolytes can alter the crystalline structure of the amphiphile chains provided they are bound. A question is raised whether the backbone structure of polyelectrolytes induces crystalline and mesomor-

* Corresponding author. Telephone: +86-20-8711-2886. Fax: +86-20-8711-0273. E-mail:mcztong@scut.edu.cn.

CDV

Table 1. Composition and Thermal Properties of *b*PEI−OA-*x* Complexes

sample	x_{feed}	N (wt %)	T_m (°C)^a	ΔH_m (J/g)^b	X_c^{OA} (%)	T_i (°C)^a
*b*PEI−OA-0.35	0.30	9.74	52.3	38.98	28.8	102.5
*b*PEI−OA-0.47	0.40	7.98	55.9	62.84	42.9	116.1
*b*PEI−OA-0.55	0.50	6.99	59.2	70.38	45.9	118.5
*b*PEI−OA-0.63	0.65	6.29	60.5	70.77	44.7	115.1
*b*PEI−OA-0.69	0.80	5.85	60.1	70.98	44.7	110.2
*b*PEI−OA-0.73	1.00	5.60	60.3	73.60	45.9	105.4

^{a} Peak values. ^{b} Melting heat of the complexes.

phous structure change in the polyelectrolyte−amphiphile complex. Up to now, however, little attention has been paid to this aspect, perhaps due to the lack of available polyelectrolytes having the same repeat unit but different backbones.

PEI is a desirable candidate polyelectrolyte because there are both linear and highly branched samples available with the same monomer unit *ethylenimine*. Therefore, we comparatively studied the crystalline structure of the bound OA tail chains and mesomorphous structure of the complexes of the branching PEI and OA having nonequimolar compositions with those of linear PEI to reveal the structure change induced by backbone branching.

2. Experimental Section

Materials. Branched poly(ethylenimine) (*b*PEI, Aldrich, M_w 25 000 g/mol), linear poly(ethylenimine) (*l*PEI, Alfa, M_w 25 000 g/mol), and octadecanoic acid (OA, Shanghai Chemical Reagent Co.) were used as received without further purification. The molar ratio of primary to secondary to tertiary amino groups is about 1:2:1 for *b*PEI according to the literature.[20] All other chemicals were analytical reagents and purified according to the standard procedures.

Complex Preparation. The complex was prepared by mixing OA and PEI in ethanol solution at about 75 °C just below its boiling temperature. As a general procedure, 2.84 g of OA was dissolved in 20 mL of ethanol at about 75 °C and the solution was slowly added dropwise into the PEI ethanol solution of equal volume under stirring for 5 h. The mixed solution was cooled to produce white solid (the solvent in the solution of $x < 0.5$ was allowed to evaporate slowly until white solid appeared), which was separated by filtration, washed three times with ethanol, and dried under vacuum for 48 h at room temperature. The nitrogen content N wt % of the complex was determined with a Vario EL elemental analyzer and the composition x (mole ratio of OA to amino group of *b*PEI) was evaluated (Table 1).

Measurements. Fourier transform infrared (FTIR) spectra of the complexes were recorded on a Bruker Vector 33 FTIR spectrometer using KBr pellets at room temperature. Wide-angle X-ray diffraction (WAXD) and small-angle X-ray scattering (SAXS) measurements of the complex powder were performed in transmission geometry with a X'pert PRO diffractometer (40 kV and 40 mA) using Cu K_α radiation (wavelength $\lambda = 0.154$ nm) at room temperature. The 2θ ranged from 10° to 30° for WAXD and the scattering vector s ranged from 0.113 to 1.55 nm^{-1} for SAXS, where $s = (2/\lambda) \sin\theta$. The scan step was 0.01° in 2θ with a counting time of 2 s/step. Differential scanning calorimetry (DSC) experiment was performed with 3−5 mg of sample in a 6 mm aluminum pan on a Netzsch DSC 204 under nitrogen atmosphere at a heating or cooling rate of 10 °C/min following the temperature sequence as room temperature → 140 °C → −60 °C → 140 °C. Thermogravimetry (TG) was carried out with a Netzsch TG 209 under nitrogen atmosphere at a heating rate of 10 °C/min starting from room temperature to 500 °C. Polarized optical microscope of Zeiss Axiophot was used with a Linkam hot stage. The sample was heated from room temperature to 140 °C and held for 3 min to remove the heat history and then cooled to room temperature and subsequently heated to
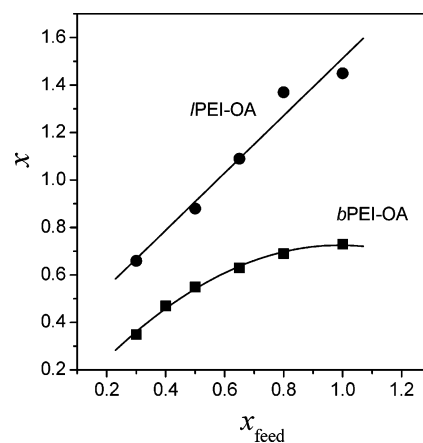

Figure 1. Plot of the actual mole ratio x of OA to amino group in PEI for the *b*PEI−OA and *l*PEI−OA complexes against the feed composition x_{feed}.

90 °C again at the rate of 10 °C/min. The photos were taken at 90 °C.

3. Results and Discussion

Complex Composition. In preparing nonequimolar polymer− amphiphile complexes, the feed mole ratio x_{feed} of OA to *b*PEI was restricted not beyond the unit value (Table 1). Plots of actual composition x of *b*PEI−OA-*x* complexes are illustrated in Figure 1 as a function of x_{feed}, compared with those for the *l*PEI− OA-*x* complexes. Interestingly, the actual composition x is always lower than x_{feed} for *b*PEI−OA-*x* complexes, especially for $x_{feed} \geq 0.8$. This is due to the difference in the basicity or the protonation degree of different amino groups in the *b*PEI backbone. Because the pK_b value in aqueous solution is 3.35, 3.27, and 4.22 for CH_3NH_2, $(CH_3)_2NH$, and $(CH_3)_3N$ at 25 °C,[21] the basicity of three kinds of amino groups is on the order of 2° > 1° > 3°. The present *b*PEI sample contains all of these three kinds of amino groups at the molar ratio of primary to secondary to tertiary amino groups as about 1:2:1.[20] The tertiary amino groups hardly form the ionic complex with weak acidic OA molecules in ethanol solution via. proton-transfer reaction from −COOH to >N− group. Therefore, once weak acid OA was dropped into an ethanol solution containing an excess of *b*PEI, the secondary amino group would be preferentially protonated and then primary to form the precipitate of nonequimolar *b*PEI−OA complex. As a result, the observed x value is always lower than 0.75 for the *b*PEI−OA-*x* complexes when $x_{feed} \leq 1$ because only secondary and primary amino groups (ca. 75 mol %) in *b*PEI can form the ionic complex with OA. In contrast, the x for the *l*PEI−OA-*x* complexes with linear PEI is much higher than that for the *b*PEI−OA-*x* complexes when compared at the same feed composition x_{feed} for the *l*PEI has only secondary amino groups all of which can form the complex with OA.[19]

The x value for the *b*PEI−OA-*x* complex is always lower than unit while for the *l*PEI−OA-*x* complex it is even higher than unit at $x_{feed} \leq 1$. This means that there are unbound or "free" OA molecules in the *l*PEI−OA-*x* complex as $x > 1$, which align parallel to the bound OA chains and cocrystallize together due to the hydrophobic interaction between their alkyl tails and hydrogen-bonding interaction between polar heads of OA molecules.[19] This denser packing is considered to be caused by more regular backbone structure of *l*PEI, compared with that of *b*PEI.

Crystallization of Bound OA Molecules. WAXD and SAXS were performed to reveal crystalline structure of the complex. CDV
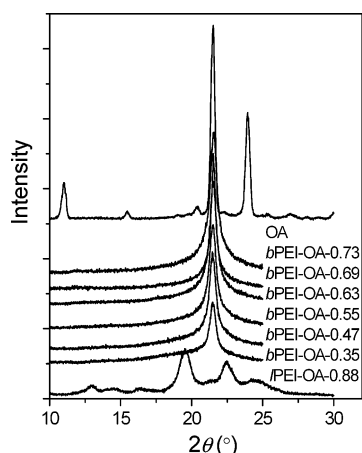
Figure 2. WAXD patterns of *b*PEI−OA-*x* complexes with indicated *x* values at room temperature compared with those of pure OA and *l*PEI−OA-0.88.

Figure 2 shows the WAXD profiles of the *b*PEI−OA complexes in the range of 2θ from 10 to 30° with those of pure OA and *l*PEI−OA-0.88 for comparison. The *b*PEI−OA complexes display only one sharp diffraction peak at $2\theta = 21.5°$ corresponding to the *d*-space of 0.41 nm, indicating the presence of the crystalline phase in the complexes. Because *b*PEI is an amorphous polymer, the crystalline structure in the *b*PEI−OA complexes is from the bound OA molecules. On the other hand, the complex *l*PEI−OA-0.88 displays three main reflections at $2\theta = 19.5, 22.5,$ and $24.6°$ corresponding to the spacing $d = 0.46, 0.39,$ and 0.36 nm. It have been reported that long aliphatic hydrocarbons can form various crystalline phases, such as hexagonal (α_H), orthorhombic (β_O), triclinic (β_T), and monoclinic (β_M) structures.[22−24] For example, the α_H structure has one main diffraction at 0.42 nm and the β_O structure shows two main diffractions at 0.42 and 0.38 nm. As for the β_T packing, there are three main diffractions at 0.45, 0.38, and 0.36 nm. According to the above discussion, pure OA corresponds to the β_O crystalline structure with two diffraction peaks at $2\theta = 21.5$ and $23.9°$ from the (110) and (200) planes for the alkyl tails.[25] In all the *b*PEI−OA complexes, the alkyl tail chains of bound OA are in the α_H phase with the (110) plane diffraction at 0.42 nm. For comparison, the *l*PEI−OA-*x* complexes are predominant with the β_T phase when $x < 1$ and dominant with the β_O phase when $x > 1$.[19]

The crystal structure of the bound alkyl tails was further verified by the FTIR spectrum in the range of around 720 cm⁻¹ associated with the CH₂ rocking mode. The orthorhombic packing β_O of the hydrocarbon chains has dual absorptions at 719 and 727 cm⁻¹, while the hexagonal α_H and triclinic β_T structures have only one band at 720 or 717 cm⁻¹, respectively.[24] The FTIR spectra in Figure 3 exhibit two absorbance bands at 718 and 727 cm⁻¹ for pure OA, indicating its β_O packing phase. All of the *b*PEI−OA complexes display only one band approximately at 720 cm⁻¹, indicating the characteristic of the α_H phase, in consistence with the WAXD results.

From the above results, we found that the crystalline structure of the bound OA alkyl tails varied from the α_H phase in the *b*PEI−OA complexes to the β_T phase in the *l*PEI−OA complexes of $x < 1$. In other words, the crystalline structure of alkyl tails bound on the polymer main chain can be altered by branching of the polymer backbone. We consider that this variation seems to be induced by the possible space supplied by the polymer backbone for the bound OA chain parking. In the *b*PEI−OA complexes, the highly branched polymer backbone increases the chain density and causes the bound OA tails
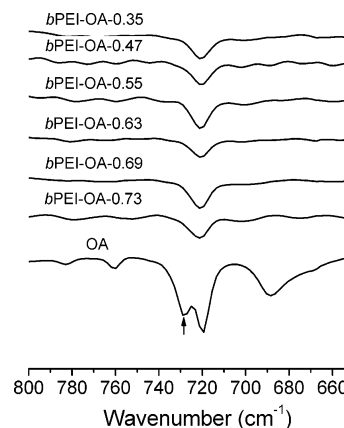

Figure 3. FTIR transmittance spectra of pure OA and *b*PEI−OA-*x* complexes at room temperature with indicated *x* values. The curves were vertically shifted to avoid overlapping.
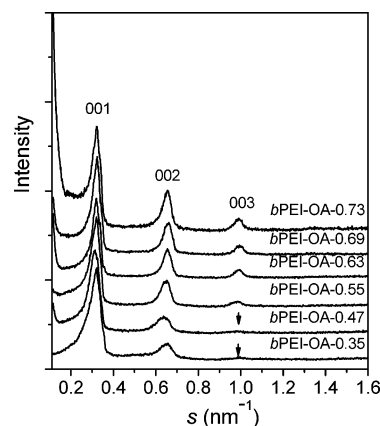

Figure 4. SAXS patterns of the *b*PEI−OA-*x* complexes at room temperature with indicated *x* values.

Table 2. SAXS *d*-Space of *b*PEI−OA-*x* Complexes

sample	d_{001}(nm)	d_{002}(nm)	d_{003}(nm)
*b*PEI−OA-0.35	3.13	1.54	1.01
*b*PEI−OA-0.47	3.21	1.56	1.03
*b*PEI−OA-0.55	3.09	1.54	1.02
*b*PEI−OA-0.63	3.13	1.52	1.00
*b*PEI−OA-0.69	3.06	1.51	1.00
*b*PEI−OA-0.73	3.11	1.52	1.00

to form a more symmetric α_H phase, compared to the less symmetric triclinic β_T phase in the *l*PEI−OA complexes of $x < 1$.[19]

Mesomorphous Structure. The SAXS patterns of the *b*PEI−OA complexes are illustrated in Figure 4. The upturns at very low *s* were due to the instrument baseline as seen in the Supporting Information. There are at least three reflections at the equidistant positions in s^{-1} scale as 1:2:3, which is the characteristic of lamellar mesomorphous structure.[3,6] The corresponding long period is about 3.1 nm from (001) reflection (Table 2). This lamella consists of a crystalline OA alkyl layer and a *b*PEI chain layer with the ionic headgroups of the amphiphiles. Because the fully extended length of an OA molecule is ~2.4 nm[26] and the polymer layer with ionic heads is ~1.4 nm,[3] the long period of 3.1 nm suggests a declined interdigitated arrangement for the alkyl tail chains in the complex. Furthermore, the strength of the third reflection becomes stronger with increasing *x*, indicating a more ordered stacking of the complex with more OA content due to the increase in packing density.
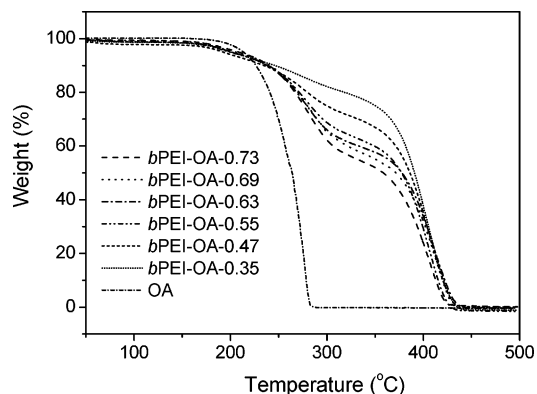
CDV

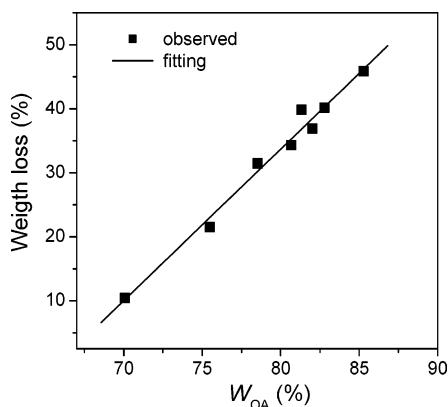**Figure 5.** TG thermograms of pure OA and *b*PEI−OA-*x* complexes with indicated *x*.

Figure 6. Relationship between the weight loss at the first maximum weight-loss and the OA weight fraction (W_{OA}) in the *b*PEI- and *l*PEI−OA-*x* complexes.

Compared with the *b*PEI−OA complexes, the SAXS patterns of the *l*PEI−OA complexes of *x* < 1 have at least four reflections at the equidistant positions in s^{-1} scale as 1:2:3:4, indicating a more ordered lamellar stacking.[19] The observed data indicate that the alkyl tails of OA in the *l*PEI−OA-*x* complexes of *x* < 1 are also interdigitated to form a denser stacking lamella than that of the *b*PEI−OA-*x* complexes.

Thermal Properties. The thermal properties of the complexes were characterized with TG and DSC. TG thermograms indicate that the *b*PEI− and *l*PEI−OA complexes are thermally stable approximately below 200 °C and exhibit a two-step weight-loss process at higher temperatures. The first maximum weight-loss occurs at 276−281 °C for the *b*PEI−OA, which is 20−25 °C higher than 255 °C for pure OA, as shown in Figure 5, indicating an enhanced thermal stability of the complexes due to the strong electrostatic interactions between −COO$^-$ from OA and −NH$_2^+$ or −NH$_3^+$ from *b*PEI. For the *l*PEI−OA complexes the temperature of the first maximum weight-loss even increases to 288−296 °C, indicating that the *l*PEI−OA complexes have a slightly higher thermal stability than the *b*PEI−OA complexes.[19] Furthermore, it is found that the total weight loss at the first-step significantly increases with increasing *x*. A good linear relationship between the weight loss at the first maximum weight-loss and the OA weight fraction in the *b*PEI−OA and *l*PEI−OA complexes (W_{OA}) was obtained with the correlation coefficient of 0.991 and standard deviation of 1.65 (Figure 6). This indicates that the first-step weight-loss is due to the partial decomposition of the OA chains bound to the PEI. The second weight-loss step at about 350 °C is due to the degradation of the PEI backbone in the complex, as reported previously.[16,18,19]
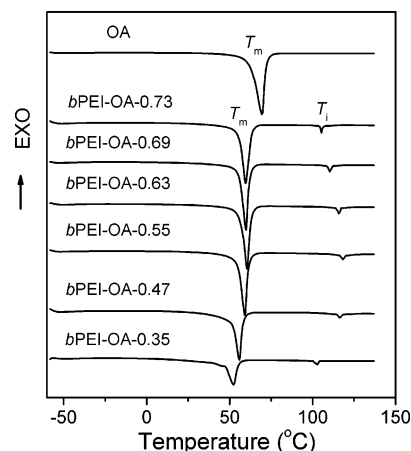

Figure 7. DSC traces of pure OA and *b*PEI−OA-*x* complexes with indicated *x* values recorded during the second heating run at the rate of 10 °C/min. The curves were vertically shifted to avoid overlapping with arbitrary scale.
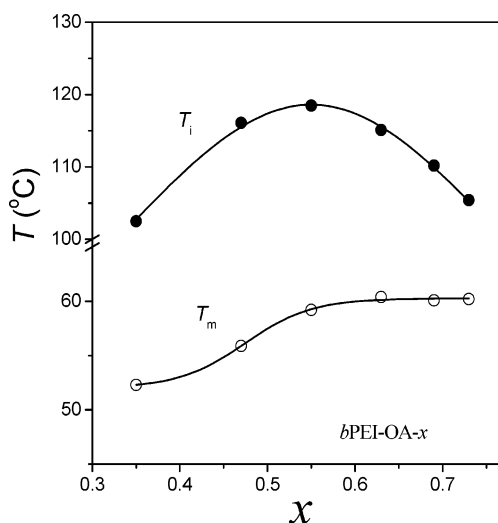

Figure 8. Melting point T_m (○) and isotropic temperature T_i (●) of the *b*PEI−OA-*x* complexes as a function of composition *x*.

DSC traces in Figure 7 indicate that there is no glass transition for the *b*PEI−OA complexes in the temperature range of −50 to +140 °C. This is consistent with that reported for the *b*PEI-carboxylate complexes (*x* = 0.5) with different alkyl side chains[13,14] and *l*PEI−OA complexes.[19] The reason for this appears to be the stiffening of polymer chains resulted from crystalline packing of the bound OA molecules, which greatly restricts the mobility of polymer chains. Furthermore, two clear endothermic transitions are observed for all the complexes in the DSC curves. The first endothermic transition is clearly due to melting the OA alkyl tail crystals of the α_H phase in *b*PEI−OA complexes, which is another evidence for the existence of crystalline phase in the complex at room temperature as observed from WAXD profiles. As depicted in Figure 8, the T_m of the α_H phase in the *b*PEI−OA complex significantly increases from 52.3 to 59.2 °C with increasing *x* from 0.35 to 0.55 and then remains almost constant. The melting point of the OA tail crystal in either *b*PEI−OA or *l*PEI−OA complexes is lower than that of pure OA, indicating that the crystal structure of bound OA chains is not so perfect as pure OA.

To determine the crystallinity of OA chains in the complex, the measured heat ΔH_m is considered as the contribution from crystal melting of the OA chains only. By roughly assuming that the crystalline CH$_2$ groups packed in the PEI−OA complexes have the same melting enthalpy, the crystallinity of
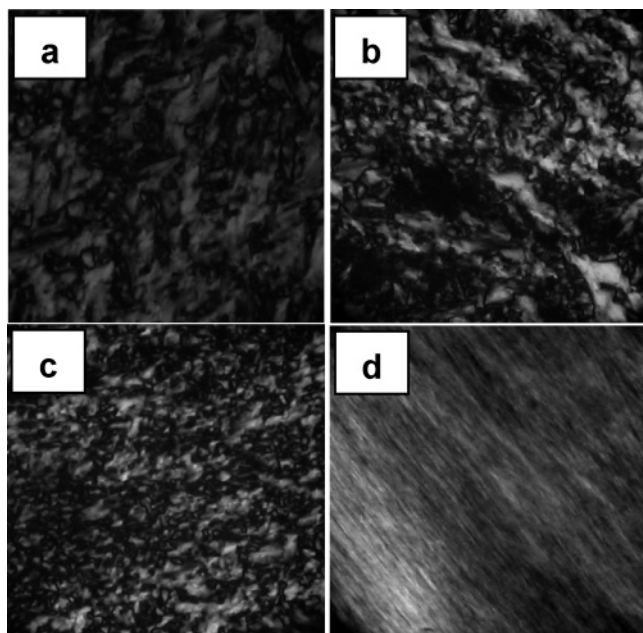
CDV

Figure 9. Polarized optical micrographs taken at 90 °C for the *b*PEI−OA complexes: (a) *b*PEI−OA-0.35; (b) *b*PEI−OA-0.55; (c) *b*PEI−OA-0.63; (d) *b*PEI−OA-0.73 after shearing.

the OA chains X_c^{OA} is determined as

$$X_c^{OA} = \frac{\Delta H_m}{\Delta H_m^{OA} W_{OA}} \qquad (1)$$

where W_{OA} is the OA weight fraction in the complexes. ΔH_m and ΔH_m^{OA} are the transition heats of the complex and pure OA, respectively. The measured ΔH_m are listed in Table 1. The ΔH_m value for the *b*PEI−OA complexes ranges 38.98−73.60 J/g, much smaller than the measured value of 194 J/g for pure OA. Consequently, the crystallinity X_c^{OA} of the bound OA chains in the *b*PEI−OA complexes is approximately estimated to be 29−46%, as shown in Table 1. It is worth noting that OA chains in the *b*PEI−OA complexes exhibit a slight increasing tendency to crystallize with increasing *x* from 0.35 to 0.55, which agrees well with the increase in T_m of the α_H crystalline phase (Figure 8) due to more regular arrangement of OA chain packing detected by SAXS (Figure 4). For the complexes *l*PEI−OA-0.66 and -0.88 with the comparable composition *x*, the X_c^{OA} is 48.0 and 48.4%, respectively,[19] indicating that the *l*PEI−OA complexes have a slightly higher crystallinity than the *b*PEI−OA. Hence, the backbone branching of PEI will reduce the crystallinity of the bound OA chains in the *b*PEI−OA complex, compared with that in the *l*PEI−OA complex having the similar OA content, though the symmetry of the crystal in the former is higher than that in the latter.

The second weak endothermic in DSC traces (Figure 7) observed at 100−120 °C for the six *b*PEI−OA complexes can be ascribed to the transition from the liquid crystalline phase to the isotropic phase. The liquid crystalline state is further verified by the polarized optical microscopy. All the *b*PEI−OA complexes exhibited birefringent fanlike textures under polarized light at 90 °C and the oriented texture was observed after being sheared in one direction at the same temperature (Figure 9). Therefore, these complexes are in the so-called ionic thermotropic liquid crystalline state in the temperature range between the T_m (the main transition) and the isotropic temperature T_i (the weak transition);[27] although pure OA never forms liquid crystalline phase. Because the SAXS patterns of the

*b*PEI−OA complexes exhibited at least three reflections at equidistant positions on the s^{-1} scale at room temperature, the liquid crystalline phase of the *b*PEI−OA complexes can be accordingly assigned as smectic B,[28] similar to the *l*PEI−OA-*x* complexes of *x* < 1. It is worth noting that the isotropic temperature T_i strongly depends not only on the polymer backbone structure (linear or branching) but also on the complex composition *x*. As seen from Figure 8, the T_i of the *b*PEI−OA complexes gradually increases from 102.5 to 118.5 °C with increasing *x* from 0.35 to 0.55 and then decreases as *x* increases further. The T_i (78−85 °C) of the *l*PEI−OA complexes is significantly lower by ∼20 °C than that (100−120 °C) of the *b*PEI−OA complexes,[19] which may be due to the lower symmetry of the β_T phase in the *l*PEI−OA side-chain crystal. Some of the ordered structure should remain in the complexes at temperatures between T_m and T_i, which seems to be the origin that the liquid crystal phase comes from.

4. Conclusions

We have found that the crystalline structure of the OA alkyl tails bound on polyelectrolytes varied with the backbone branching of the polyelectrolyte: the α_H phase for branched PEI, in contrast to the β_T phase for linear PEI when *x* < 1.0. The partial crystalline OA alkyl phase combines with polyelectrolyte-ionic head layer to form a lamellar stacking mesomorphous structure with the long period of about 3.1 nm for the *b*PEI−OA complexes, longer than 2.8 nm for the *l*PEI−OA complexes. Interestingly, a ionic thermotropic liquid crystal state, i.e., smectic B, has been found in all *b*PEI−OA complexes investigated at temperatures above the melting point of the OA tail crystal and the isotropic transition temperature T_i of these complexes is ∼20 °C higher than that for the *l*PEI−OA-*x* complexes of *x* < 1 due to the higher symmetry of the α_H phase in the *b*PEI−OA complexes. This study demonstrates for the first time that in addition to the complex composition the backbone structure (linear or branch) of polyelectrolytes plays an important role in determining the crystalline and mesomorphous structures of the polyelectrolyte−amphiphile complex.

Supporting Information Available: A figure showing the comparison of SAXD profiles for the complex sample *b*PEI−OA-0.73 and blank sample holder. This material is available free of charge via the Internet at http://pubs.acs.org.

References and Notes

(1) Zhou, S.; Chu, B. *Adv. Mater.* **2000**, *12*, 545.

(2) Ikkala, O.; Brinke, G. T. *Science* **2002**, *295*, 2407.

(3) Antonietti, M.; Conrad, J.; Thünemann, A. *Macromolecules* **1994**, *27*, 6007.

(4) Ruokolainen, J.; Tanner, J.; ten Brinke, G.; Ikkala, O.; Torkkeli, M.; Serimaa, R. *Macromolecules* **1995**, *28*, 7779.

(5) Chen, L.; Xu, S.; McBranch, D.; Whitten, D. *J. Am. Chem. Soc.* **2000**, *122*, 9302.

(6) Thünemann, A. F. *Prog. Polym. Sci.* **2002**, *27*, 1473.

(7) Thünemann, A. F.; Ruppelt, D.; Schnablegger, H.; Blaul, J. *Macromolecules* **2000**, *33*, 2124.

(8) Faul, C. F. J.; Antonietti, M. *Adv. Mater.* **2003**, *15*, 673.

(9) Talsma, S. S.; Babensee, J. E.; Murthy, N.; Williams, I. R. *J. Controlled Release* **2006**, *112*, 271.

(10) Vieira, M.; Tavares, C. R.; Bergamasco, R.; Petrus, J. C. C. *J. Membr. Sci.* **2001**, *194*, 273.

(11) Dai, J.; Bruening, M. L. *Nano Lett.* **2002**; *2*, 497.

(12) Hwang, M.-J.; Kim, K. *Langmuir* **1999**, *15*, 3563.

(13) Ujiie, S.; Takagi, S.; Sato, M. *High Perform. Polym.* **1998**, *10*, 139.

(14) Thünemann, A. F.; General, S. *Langmuir* **2000**, *16*, 9634.

(15) Thünemann, A. F. *Langmuir*, **2000**, *16*, 824.

(16) Chen, H.-L.; Hsiao, M.-S. *Macromolecules* **1999**, *32*, 2967.

(17) Zhou, S.; Zhao, Y.; Cai, Y.; Wang, D.; Xu, D. *Chem. Commun.* **2003**, 1932.

(18) Ren, B.; Tong, Z.; Liu, X.; Wang, C.; Zeng, F. *Langmuir* **2004**, *20*, 10737.

(19) Ren, B.; Cheng, Z.; Tong, Z.; Liu, X.; Wang, C.; Zeng, F. *Macromolecules* **2005**, *38*, 5675.

(20) Thomas, M.; Klibanov, A. M. *Proc. Natl. Acad. Sci. U.S.A.* **2002**, *99*, 14640.

(21) Morrison, R. T.; Boyd, R. N. *Organic Chemistry*, 4th ed.; Allyn and Bacon: Boston, 1983; pp 887−889.

(22) Bazuin, C. G.; Brodin, C. *Macromolecules* **2004**, *37*, 9366.

(23) Lee, J. L.; Pearce, E. M.; Kwei, T. K. *Macromolecules* **1997**, *30*, 6877.

(24) Luyten, M. C.; Alberda van Ekenstein, G. O. R.; ten Brinke, G.; Ruokolainen, J.; Ikkala, O.; Torkkeli, M.; Serimaa, R. *Macromolecules* **1999**, *32*, 4404.

(25) Rastogi, A.; Hobbs, J. K.; Rastogi, S. *Macromolecules* **1999**, *35*, 5861.

(26) Cai, Y.; Wang, D.; Hu, X.; Xu, Y.; Zhao, Y.; Wu, J.; Xu, D. *Macromol. Rapid Commun.* **2001**, *22*, 504.

(27) Binnemans, K. *Chem. Rev.* **2005**, *105*, 4148.

(28) Oishi, Y.; Suzuki, T.; Awano, H.; Yonetake, K. *IEEE Trans. Appl. Supercond.* **2004**, *14*, 1604.